GCAGS JOURNAL
A Publication of the Gulf Coast Association of Geological Societies
www.gcags.org

Scanning Electron Microscope Petrographic Differentiation among Different Types of Pores Associated with Organic Matter in Mudrocks

Robert M. Reed, Robert G. Loucks, and Lucy T. Ko

Bureau of Economic Geology, Jackson School of Geosciences, University of Texas at Austin, University Station, Box X, Austin, Texas 78713–8924, U.S.A.

ABSTRACT

At least six distinct types of pores associated with organic matter exist in organic-matter-bearing mudrocks. Inherited (predepositional) pores are common in organic matter derived from terrestrial sources. Subgrain (granular) pores are a generally rare pore type that may have formed prior to deposition, but the pores have a distinctly different (three-sided) morphology from inherited pores. Modified mineral pores are original mineral pores that have been only partly occluded by migrated bitumen. Bubble pores are relatively large pores (up to 1 µm in diameter) that form in organic matter during thermal maturation, commonly by amalgamation of smaller bubble pores. Nanometer-scale spongy pores also form during thermal maturation, but at higher temperatures than bubble pores. Elongate dissolution pores surrounded by organic matter are thought to be unrelated to dissolution of the organic matter, but, instead, to dissolution of clay minerals intermixed in the organic matter. Very few of the microfractures seen in organic matter are thought to form naturally in the subsurface but are artifacts formed during coring or post coring. Those microfractures that clearly do form in the subsurface are made of interconnected bubble pores.

Inherited and modified mineral pores are thought to be unconnected to the overall pore system of the rock. Subgrain pores are connected in the organic-matter grain and may connect externally, but are generally not common enough to be important to the overall pore system. Dissolution pores in organic matter may contribute to storage, but not necessarily to flow. Bubble and spongy pores do appear to be commonly connected and would then be important to flow and storage of hydrocarbons.

INTRODUCTION

A classification of pore types in mudrocks that divides pores between mineral and organic-matter pores was developed by Loucks et al. (2012). Mineral pores were subdivided into interparticle (between particles) pores and intraparticle (within grains or domains) pores. Organic-matter pores were neither subdivided into pore subtypes nor according to whether they formed in kerogen or bitumen. Abundant data have been collected about the range of organic-matter pore morphologies and distributions by the authors and numerous other workers (e.g., Katz and Arango, 2018, and references therein). Previous workers (e.g., Driskill et al., 2012, 2013; Jennings and Antia, 2013) have proposed classifications of organic-matter pores primarily on the basis of morphology. A classification of organic-matter pores based on the authors' examination of numerous mudrock units was the major objective of this investigation. Using petrographic examination of scanning electron microscope (SEM) images, we found that at least six distinct types of pores in organic matter can be differentiated on the basis of their morphology and apparent association with specific organic matter types.

Several reasons can be given for why the existence of multiple pore types hosted in organic matter is important. As will be discussed later, these pore types result from different formation mechanisms and they form during different periods of the organic matter's thermal history. The connectivity of these pores and the fluid(s) they contain are controlled by how and when they formed. Some of these pore types are tied to either kerogen or solid bitumen allowing a general differentiation of these two organic-matter types. Also, many recent studies (e.g., Yang et al., 2014; Liu et al., 2015) have discussed the fractal geometry of pores in organic-rich mudrocks. If these pores represent different generations, the results of these fractal studies would require different interpretations because the resulting patterns are unrelated to a single contemporaneous process.

SAMPLES AND METHODS

This study is the result of more than 13 years of examination of pores in organic matter (e.g., Reed and Loucks, 2007). During this time, more than 20 different rock units have been character-

Manuscript received April 29, 2020; revised manuscript received July 16, 2020; manuscript accepted July 20, 2020.

GCAGS Journal, v. 9 (2020), p. 17–27.

ized including major hydrocarbon-bearing units such as the Mississippian Barnett Shale (Loucks et al., 2009; Reed et al., 2014; Reed and Loucks, 2015), the Pennsylvanian Cline Shale (Reed and Roush, 2016), the Permian Wolfcamp Formation, and the Upper Cretaceous Eagle Ford Group (Ko et al., 2016, 2017; Reed et al., 2019). Hundreds of samples have been prepared using Ar–ion milling for examination in the SEM. Samples include a broad spectrum of lithologies from calcareous mudstones to argillaceous mudstones to siliceous mudstones. Samples are from a broad range of thermal maturities ranging between 0.3% vitrinite reflectance (R_o) East Texas terrestrial shales to near 2.0% R_o Fort Worth Basin Barnett Shale samples. Thermal maturities given for samples are primarily calculated R_o values based on T_{max} derived from programmed pyrolysis, with a few samples from lower thermal maturities having measured vitrinite R_o values (Reed, 2017).

Organic-matter pores were examined primarily using an FEI Nova NanoSEM 430 at low to moderate beam energies (5–15 kV) on Ar–ion milled surfaces. Samples were prepared using three different Ar–ion milling systems—a Gatan PECS with slope cutter attachment, a Leica TIC020, and a Leica TIC3X. Both backscattered electron and secondary electron images were acquired of porous areas to provide a full picture of pore features. Associated energy dispersive spectroscopy element maps captured and provided identification of mineral phases accompanying organic matter.

OBSERVATIONS AND ORIGINS OF PORE TYPES

Pore types are described next in interpreted order of timing of formation relative to deposition and thermal maturation. Different pores types have somewhat different shapes, sizes and distributions. Some pore types occur in kerogen, some in solid bitumen or pyrobitumen, and others in either type of organic matter. The terms kerogen and bitumen are being used in an SEM petrographic sense, as discussed in Loucks and Reed (2014). Solid bitumen and pyrobitumen are impossible to differentiate using the SEM, therefore they are not treated separately here.

Inherited Organic-Matter Pores

The first pore type to be discussed consists of inherited (predepositional) organic-matter pores (Fig. 1). These pores can be highly variable in size (nanometers to micrometers) and shape (spherical to cubic to highly irregular). Inherited pores occur only in kerogen grains. In some cases, inherited pores show a number of different patterned distributions (e.g., Fig. 1A). Inherited pores are observed to be more common in grains interpreted to be type III kerogen (Figs. 1A and 1C) and are noticeably rare in samples with abundant amorphous organic matter (AOM) as the principal kerogen. These pores are susceptible to later infilling, either with migrated organic matter (bitumen) (Fig. 1A) or with diagenetic minerals (e.g., Fig. 1D or Schieber [1996]), or with very fine-grained mineral grains similar to those of the matrix.

The size, shape, and distribution of inherited pores are controlled by biological processes during plant or algal growth, accounting for the diverse morphologies found. Inherited pores are abundant in an organic-rich shale from the terrestrial Eocene Wilcox Group of East Texas (Reed, 2017). Large inherited pores are integral to organic petrographers classifying macerals as semi-fusinite and fusinite (e.g., Papp et al., 1998). Milliken et al. (2014) noted inherited pores in some organic-matter grains from low-thermal-maturity Mediterranean sapropels. The pores in kerogen noted in Fishman et al. (2012) are possibly inherited pores, as discussed in that article.

Subgrain Pores in Organic Matter

Another type are the pores found between spherical subgrains of organic matter that comprise larger, up to silt-size, kerogen grains. Variability occurs in the size of the subgrains of organic matter in different units from tens to hundreds of nanometers. Subgrain (granular) organic-matter pores are generally nanometer-scale and commonly show a three-sided morphology controlled by the spherical subgrains (Fig. 2). These subgrain pores can be hundreds of nanometers if subgrains are from the larger end of the size range (Fig. 2C). Subgrain pores are common thus far only in relatively low thermal maturity (<0.8% R_o) samples of the Pennsylvanian Smithwick Formation from the southern Fort Worth Basin (Reed, 2017). These pores have also been noted as rare occurrences in other units including the Upper Cretaceous Eagle Ford Group in low thermal maturity samples from north central Texas (Loucks et al., 2019). Reed (2017) it was suggested that these subgrain pores become more difficult to distinguish with increasing thermal maturity (Fig. 2D), although currently this observation remains speculative. It is notable that where seen at higher thermal maturities (Figs. 2B and 2D), the organic matter that makes up the subgrains does not develop other types of organic-matter pores such as spongy pores.

Whether these pores are strictly predepositional, related to microbial action, or the result of early thermal maturation of particularly labile organic matter is unclear. Possible origins for these pores were discussed more completely by Reed (2017). Regardless of their origin, these subgrain pores represent a pore morphology distinctly different from those of the inherited pores.

Modified Mineral Pores

These are relatively large (up to micrometer scale) pores found in some bitumen that has solidified (Fig. 3). These were described variously as *mineral interface pores* by Pommer and Milliken (2015), *modified mineral pores* by Ko et al. (2016, 2017) and *early bitumen pores* by Reed et al. (2019). The most common shape of these pores is spherical, but hemispheres are observed where these pores formed at the interface of the bitumen and mineral grains. These pores tend to occur as only one or two pores in the original mineral pore space. Modified mineral pores are commonly micrometer-scale although they may be smaller if the original mineral pore was small. The organic-matter walls of modified mineral pores are generally smooth. Chambers of foraminifera and the interiors of intact coccoliths are common places in which to find these pores developed (Fig. 3).

Modified mineral pores are postulated to form when migrating mobile bitumen moves into preexisting interparticle or intraparticle pores that are filled with formation water. If the bitumen fails to displace all the formation water a large pore can form either in the center (Figs. 3A, 3B, and 3D) or on the edge (Fig. 3C) of the original mineral pores. Additional maturation transposes the bitumen to solid bitumen and preserves the pores. These pores can form at relatively low thermal maturities prior to the formation of most other bitumen pore types but do persist to higher thermal maturities. As shown from the examples in Figure 3, depending on the sulfur content of the original kerogen which controls onset of bitumen formation (Orr, 1986), these pores can form at quite low maturities.

Bubble Organic-Matter Pores

Bubble pores in organic matter are a common organic-matter pore type. These pores are tens to hundreds of nanometers in diameter (Fig. 4). Initial shapes appear to be relatively spherical, although visual evidence shows that as these pores grow, they tend to merge with other pores of this type, making a more elongate and irregular composite pore (Fig. 4B). In many cases, the

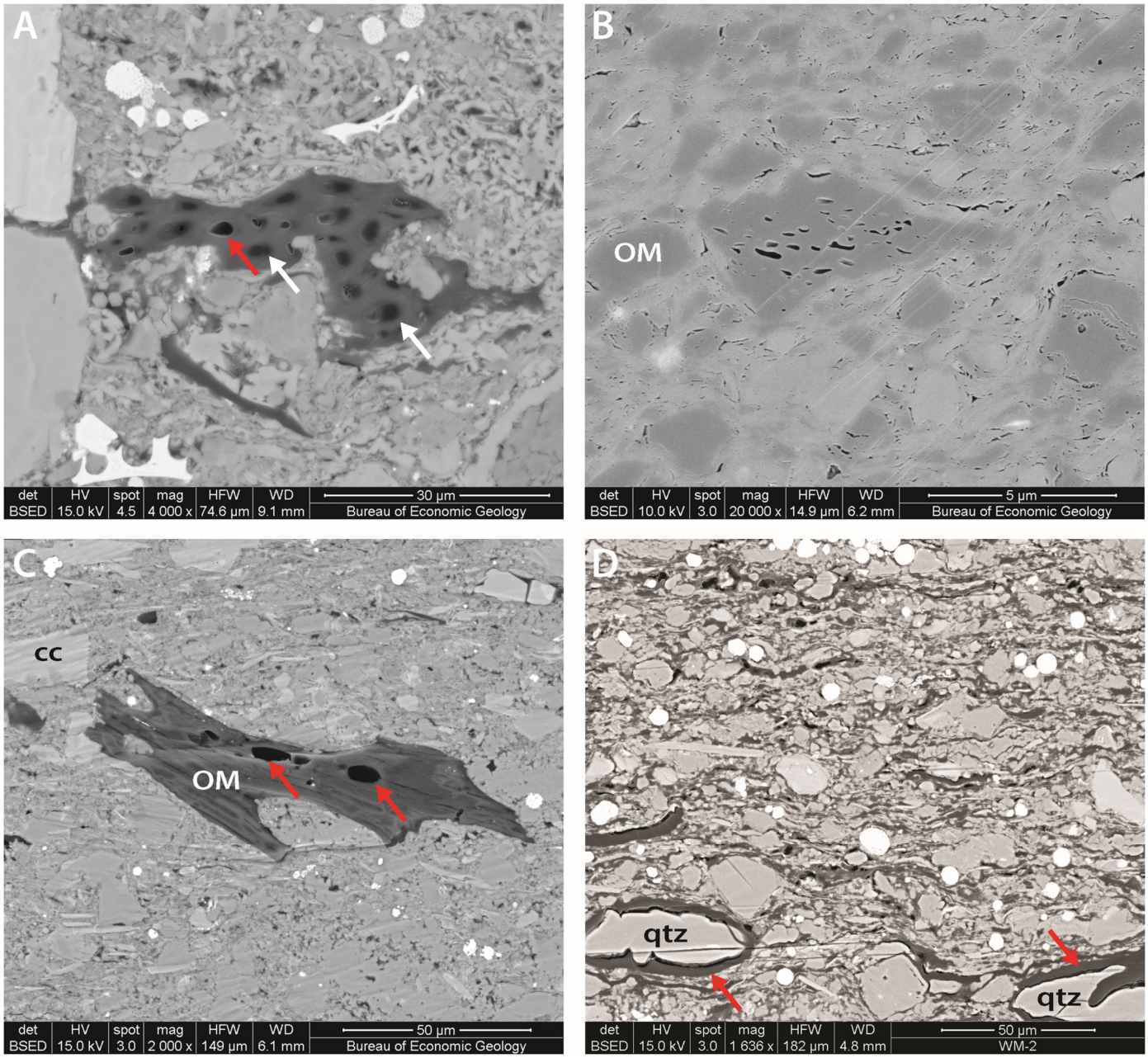

Figure 1. Backscattered electron SEM images of inherited (predepositional) pores in organic matter (OM). (A) Kerogen grain (center, black) showing inherited pores in organic matter. Red arrow points toward an open pore in the kerogen. White arrows point toward pores filled with bitumen related to thermal maturation. Upper Cretaceous Eagle Ford Group, Atascosa County, Texas, calculated R_o = ~1.1%. (B) Large organic-matter grain at center showing inherited pores. Paleogene Wilcox Group, Leon County, Texas, R_o = ~0.3%. (C) Woody grain of organic matter showing open inherited pores (red arrows). Permian Wolfcamp Shale, Reeves County, Texas, calculated R_o = ~0.9%. (D) Algal spores (red arrows) filled with recrystallized quartz (qtz). Immature Woodford Shale, southern Arbuckle Mountains, Oklahoma.

walls of these organic-matter pores are rugose and this irregularity suggests some change in the organic-matter structure (Figs. 4B and 5A). Bubbles pores are common in solid bitumen and may form in thermally altered kerogen as well (see later discussion; Fig. 4C).

We think that bubble organic-matter pores are a variety of thermal-maturation-related pores. These pores are noted to begin to appear around 0.75% R_o, in association with oil generation, although this thermal-maturity level will vary somewhat depending on the lability of the organic matter.

Spongy Organic-Matter Pores

Another common type of pores is spongy pores in organic matter (Loucks and Reed, 2014). These are nanometer-scale pores and the smallest organic-matter pores visible in the SEM (Fig. 5). On the basis of nitrogen-absorption data showing pores at sizes too small to be visible in our SEM, researchers speculated (Milliken et al., 2013) that these pores can be as small as 1 nm in diameter. Spongy pores are typically found in solid bitumen or pyrobitumen, and have spherical to irregular shapes. These

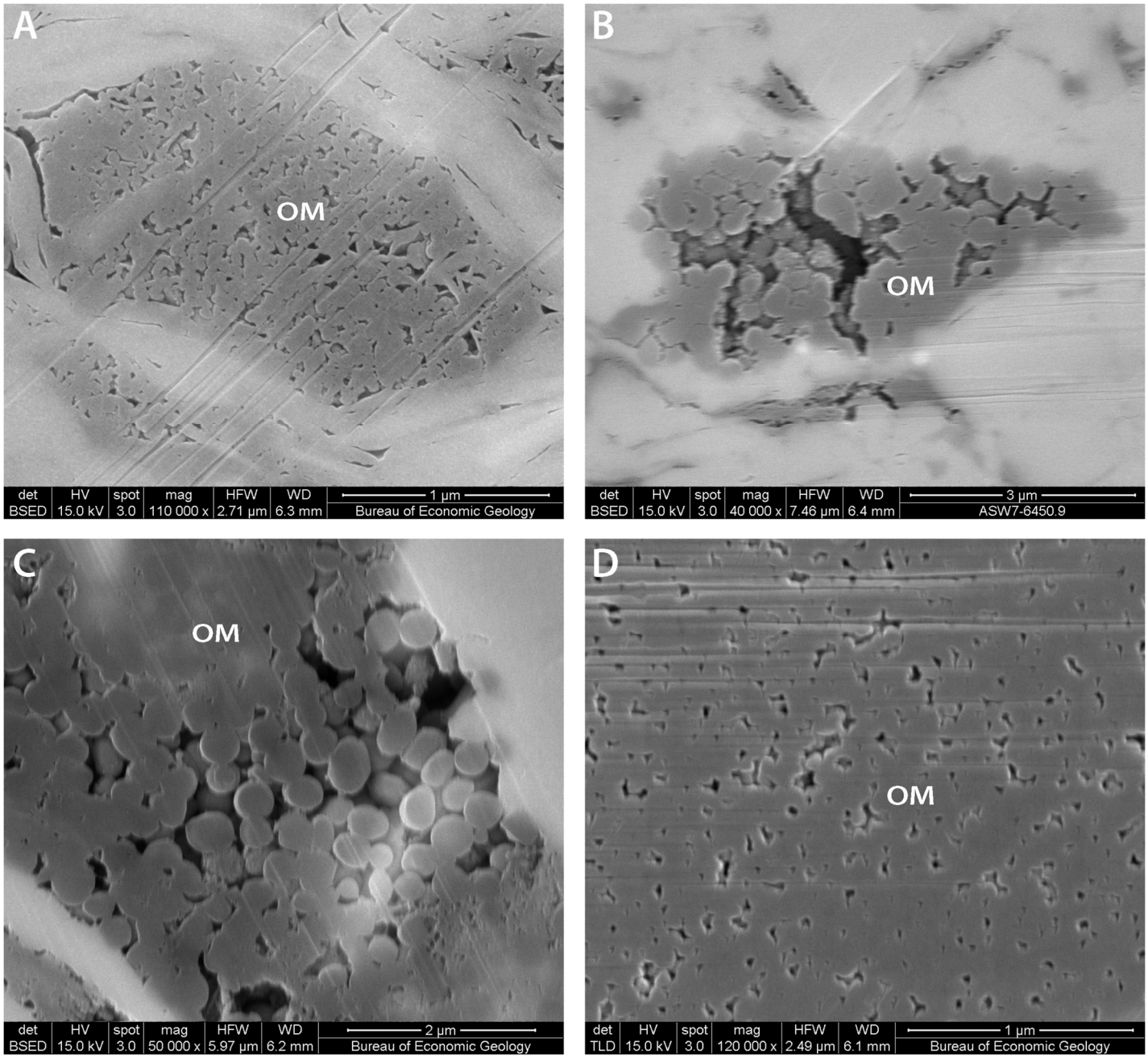

Figure 2. SEM images of subgrain (granular) pores in organic matter. (A) Organic matter grain with pores in between the smaller subgrains of organic matter comprising the larger overall grain. Pennsylvanian Smithwick Shale, McCulloch County, Texas, calculated R_o = ~0.65%. (B) Organic matter (OM) grain composed of spherical subgrains of organic matter with pores in between the spheres. Mississippian Barnett Shale, Wise County, Texas, calculated R_o = ~1.1%. (C) Close up SEM image of the smaller subgrains separated by pores making up a larger organic matter grain. Miocene Monterey Shale, California, R_o estimated to be 0.4% on the basis of mineralogy using Miki et al. (1991). (D) Secondary electron SEM image focused on the interior of an organic-matter grain that is composed of smaller subgrains. Pennsylvanian Cline Shale, Glasscock County, Texas, calculated R_o = ~0.88%.

pores can commonly be seen in the walls of the larger and earlier formed bubble pores (Figs. 4B and 5A).

Similar to bubble pores, spongy pores are interpreted to be a variety of thermal-maturation-related pores. Spongy pores begin to appear in bitumen at R_o's generally greater than 1.0%, at conditions associated with gas generation. Similar appearing pores form in some kerogen at higher thermal maturities (<1.2% R_o) and might be considered spongy pores.

Dissolution Pores Hosted by Organic Matter

The final proposed variety of pores in organic matter is associated with dissolved or partially dissolved clay minerals or micas. These clay-mineral-associated pores are elongate, and they typically have high aspect ratios (Fig. 6). Lengths can be up to several micrometers. These pores are seen in both kerogen and solid bitumen, although they are more common in bitumen.

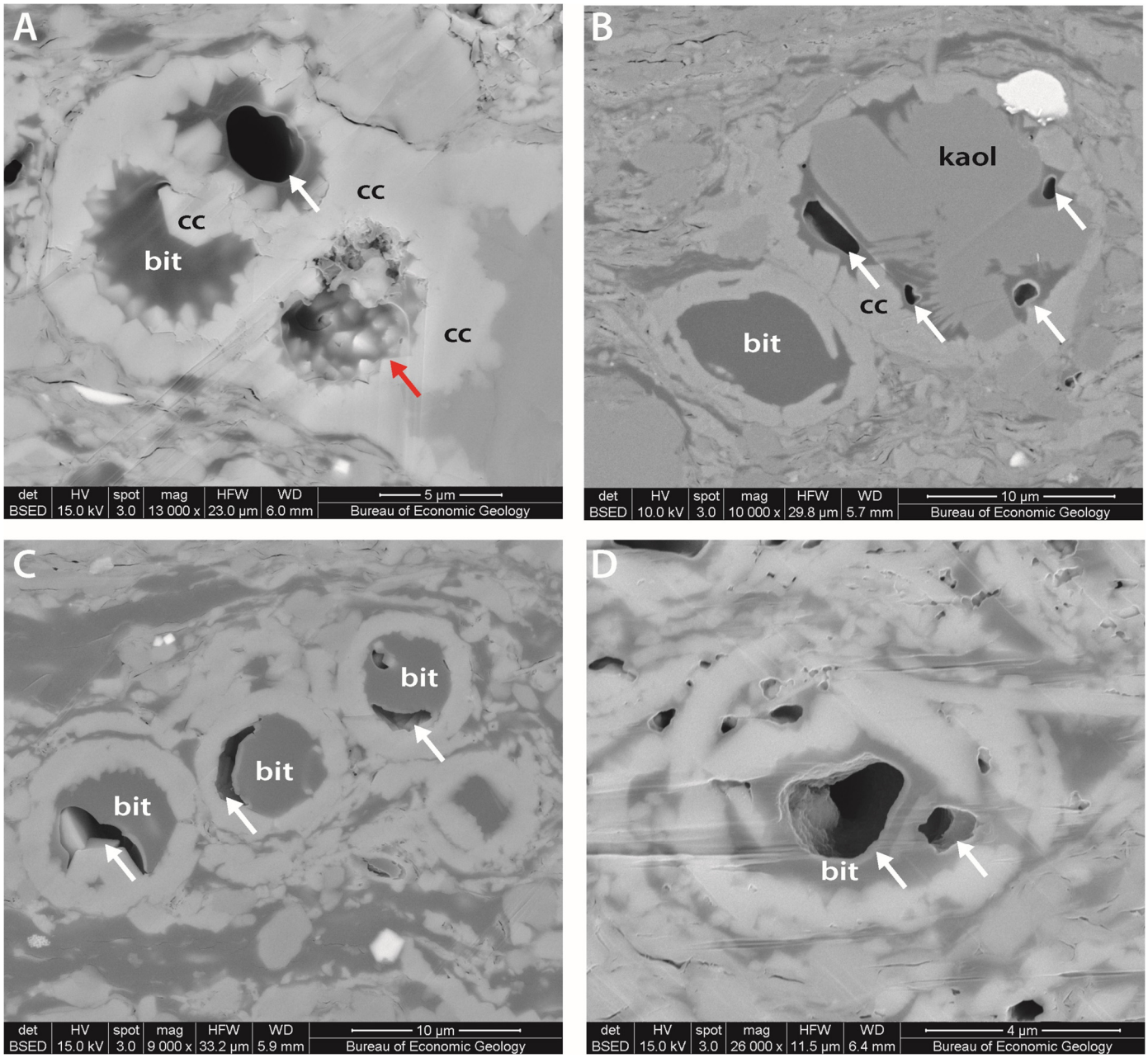

Figure 3. Backscattered electron SEM images of modified mineral pores in bitumen (bit). (A) Early bitumen or modified mineral pores in chambers of a foraminifer test. White arrow points toward spherical pore in a chamber with larger amount of bitumen (bit). Red arrow points toward irregular pore containing calcite (cc) mineralization. Upper Cretaceous Eagle Ford Group, Gonzales County, Texas, R_o = ~0.48%. (B) Modified mineral pores (white arrows) in calcisphere (?) partly filled with kaolinite (kaol). Upper Cretaceous Eagle Ford Group, Wilson County, Texas, calculated R_o = ~0.45%. (C) Intact coccoliths filled with bitumen showing modified mineral pores (white arrows) on the edges rather than centers of the original pore spaces. Upper Cretaceous Eagle Ford Group, Gonzales County, Texas, R_o = ~0.48%. (D) Partly intact coccolithophore filled with bitumen showing modified mineral pores. Upper Cretaceous Eagle Ford Group, Gonzales County, Texas, R_o = ~0.48%.

We propose one scenario by which these pores can be formed. In some situations, organic matter can become intermixed with clay minerals. In kerogen this intermixture can occur with amorphous organic matter in algal mats or marine snow. In bitumen this intermixture can occur when original mica or clay mineral grains have intraparticle pore space (e.g., expanded clays) that is subsequently filled with bitumen. When thermal stress increases with burial, some clay minerals become unstable, and recrystallize to other clay minerals (e.g., smectite going to illite, or kaolinite going to chlorite; see Milliken [2005], and references therein). This transformation can leave voids surrounded by organic matter (Fig. 6). In actuality these are dissolution pores that happen to be hosted by organic matter rather than pores that are developed by organic matter.

Microfractures in Organic Matter

Additionally, there are the problems of interpreting the origin of microfractures found in organic matter and whether these microfractures should be considered a distinct pore type.

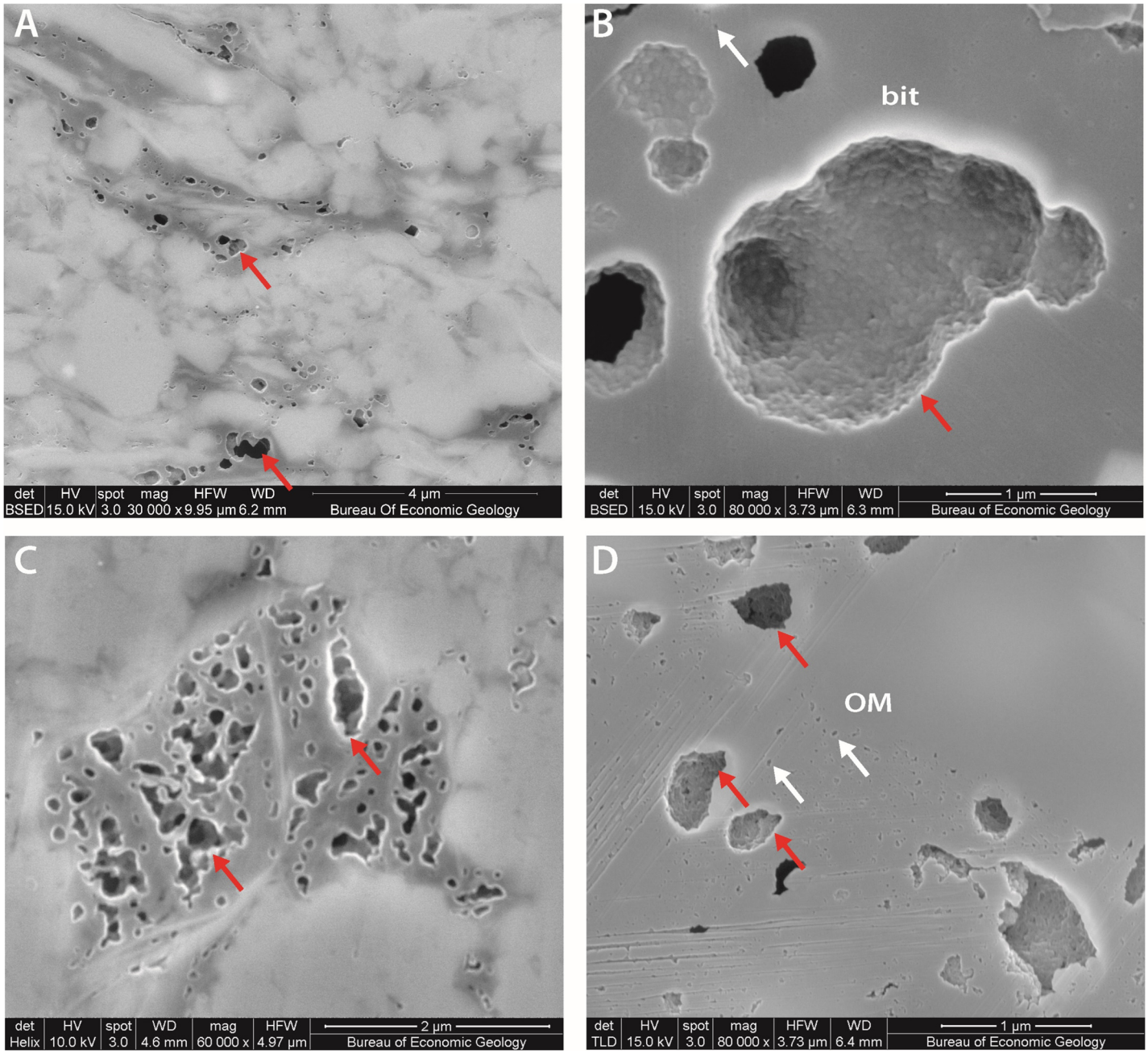

Figure 4. SEM images of bubble organic-matter pores. (A) Abundant bubble pores (red arrows) in organic matter. At lower thermal maturity of ~0.88% R_o, there are no accompanying spongy pores. Pennsylvanian Cline Shale, Glasscock County, Texas, calculated R_o = ~0.88%. (B) Bubble pores in bitumen (bit) filling foraminifer chamber. Note that the largest irregular bubble pore (red arrow) is an amalgamation of several smaller spherical pores. Small spongy pores (white arrow) also present. Upper Cretaceous Eagle Ford Group, Atascosa County, Texas, calculated R_o = ~1.1%. (C) Numerous bubble pores (red arrows) in kerogen grain. Mississippian Barnett Shale, Wise County, Texas, calculated R_o = ~1.9%. (D) Mix of bubble pores (red arrows) and spongy pores (white arrows) in organic-matter-rich (OM) part of sample. Pennsylvanian Cline Shale, Reagan County, Texas, calculated R_o = ~0.98%.

Microfractures in organic matter appear to have two general morphologies, which are probably connected to different formation mechanisms. Microfractures made of linearly connected subspherical bubble pores are an uncommon observation (Fig. 7A). These typically occur one per organic-matter mass and do not extend beyond the organic matter in which they formed. More typical straight-sided microfractures have also been observed in some organic matter (Fig. 7B). These cracks are typically observed in material interpreted to be solid bitumen, commonly with more than one crack per bitumen mass. These cracks also generally do not extend beyond the organic-matter mass in which they formed.

A common hypothesis is that the straight-sided cracks form through devolatilization of the solid bitumen (Loucks and Reed, 2016). However, whether this devolatilization occurs in the subsurface or at the surface remains unclear. Many of these micro-

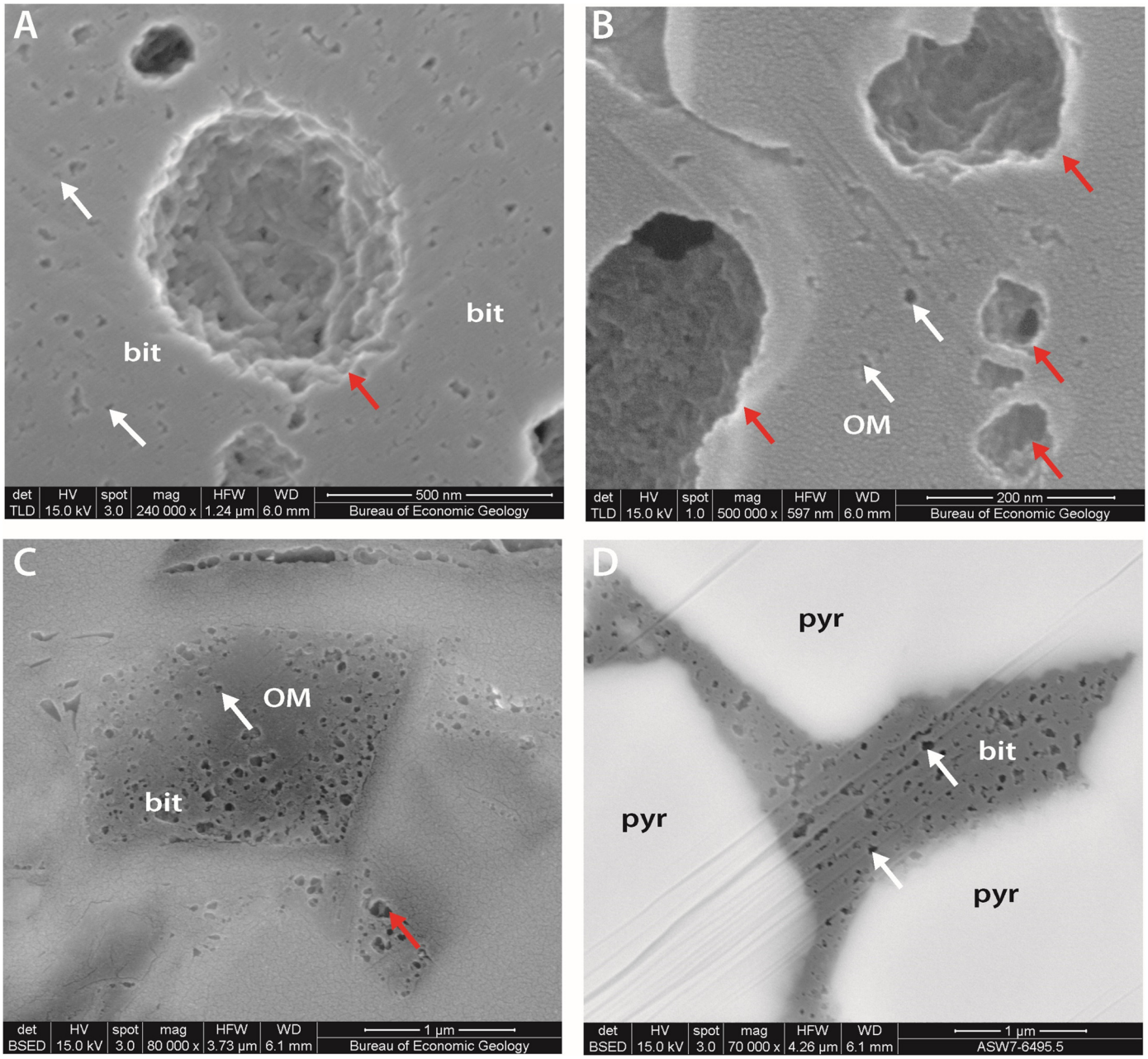

Figure 5. SEM images of spongy organic-matter pores. (A) Abundant nanometer-scale spongy pores (white arrows) with a few larger bubble pores (red arrow). Bitumen (bit) from within chamber of a foraminifer. Upper Cretaceous Eagle Ford Group, Atascosa County, Texas, calculated R_o = ~1.1%. (B) High-magnification image of an organic-matter mass with small spongy pores (white arrows) and a few larger bubble pores (red arrows). Permian Wolfcamp Shale, Reeves County, Texas, calculated R_o = ~0.9%. (C) Mix of spongy pores (white arrow) and a few slightly larger bubble pores (red arrow) in organic matter. Devonian-Mississippian New Albany Shale, Sullivan County, Indiana, calculated R_o = ~0.8%. (D) Spongy pores (white arrows) in bitumen (bit) between the microcrystals of a pyrite (pyr) framboid. Mississippian Barnett Shale, Wise County, Texas, calculated R_o = ~1.1%.

fractures have morphologies reminiscent of mudcracks (Fig. 7B), suggesting formation in a low stress environment such as at the surface.

DISCUSSION

Connectivity of Pore Types

Different types of pores will have different degrees of connectivity to larger, millimeter-scale, pore systems. In terms of storage and flow of hydrocarbons, only bubble and spongy pores are generally common enough to be considered important in most units. Numerous focused-ion-beam (FIB) studies have addressed connectivity of bubble and spongy pores in organic matter (e.g., Curtis et al., 2010, 2011, 2014). Work using tracer (spontaneous) imbibition and microcomputed tomography suggests that some bubble and spongy organic-matter pores are connected to the millimeter-scale pore system in the rock (Peng et al., 2019).

Inherited pores that remain open at higher thermal maturities in particular are thought not to have much connectivity to the

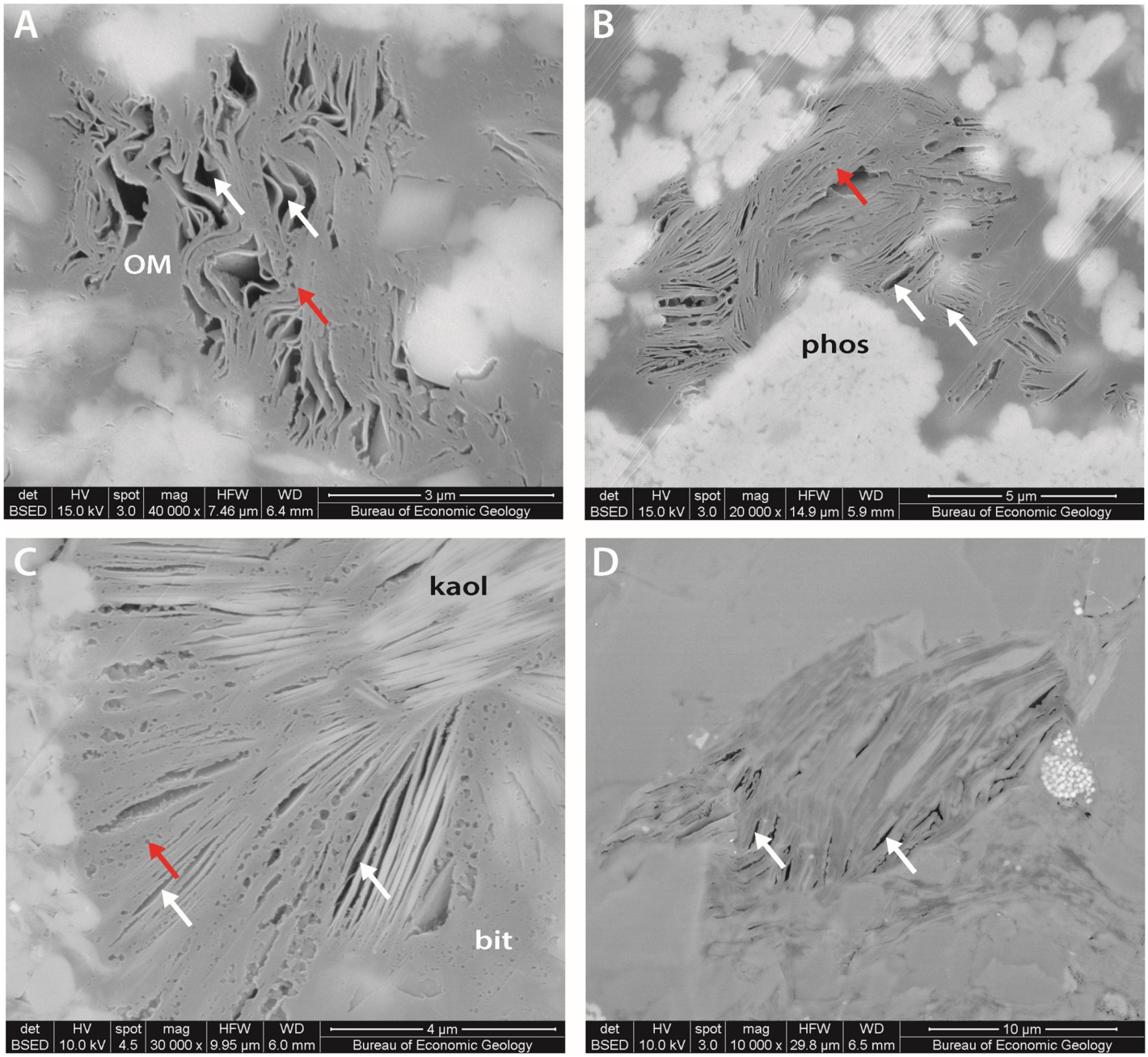

Figure 6. Backscattered electron SEM images of clay-shaped dissolution pores in organic matter (all darkest regions in images). (A) Clay-associated dissolution pores (white arrows) in organic matter. Organic matter also contains small spongy pores. Jurassic-Cretaceous Vaca Muerta Shale, Neuquén Basin, Argentina, late oil-window maturity. (B) Elongate, clay-associated organic-matter pores in bitumen (white arrows) also showing abundant circular, spongy pores in a phosphate-rich (phos) area. Mississippian Barnett Shale, Wise County, Texas, calculated R_o = ~1.1%. (C) Dissolution pores (white arrows) associated with kaolinite (kaol) in a bitumen (bit) mass. Organic matter also contains some spongy (red arrow) and bubble pores. Jurassic-Cretaceous Vaca Muerta Shale, Neuquén Basin, Argentina, calculated R_o = ~0.9%. (D) Dissolution pores (white arrows) in organic matter grain. Permian Bone Spring Formation, Reeves County, Texas, calculated R_o = ~0.9%.

overall pore system of the rock. Those that do have connectivity to outside the organic-matter grain are commonly filled with migrated bitumen (Fig. 1A) or diagenetic minerals (Fig. 1D).

Modified mineral pores do not seem to be connected to the larger pore system after their formation. Otherwise they, like inherited pores, would be susceptible to later infilling by diagenetic minerals.

Dissolution pores in organic matter (Fig. 6) should be connected to the overall pore system in the rock. The proposed formation mechanism requires a connection for the necessary chemical reactions to have occurred. This explains why these pores are typically more abundant near the edges of the organic-matter masses in which they formed.

Challenges in Pore Type Differentiation

Several of these organic-matter pore types present challenges in differentiating them from other types of organic-matter

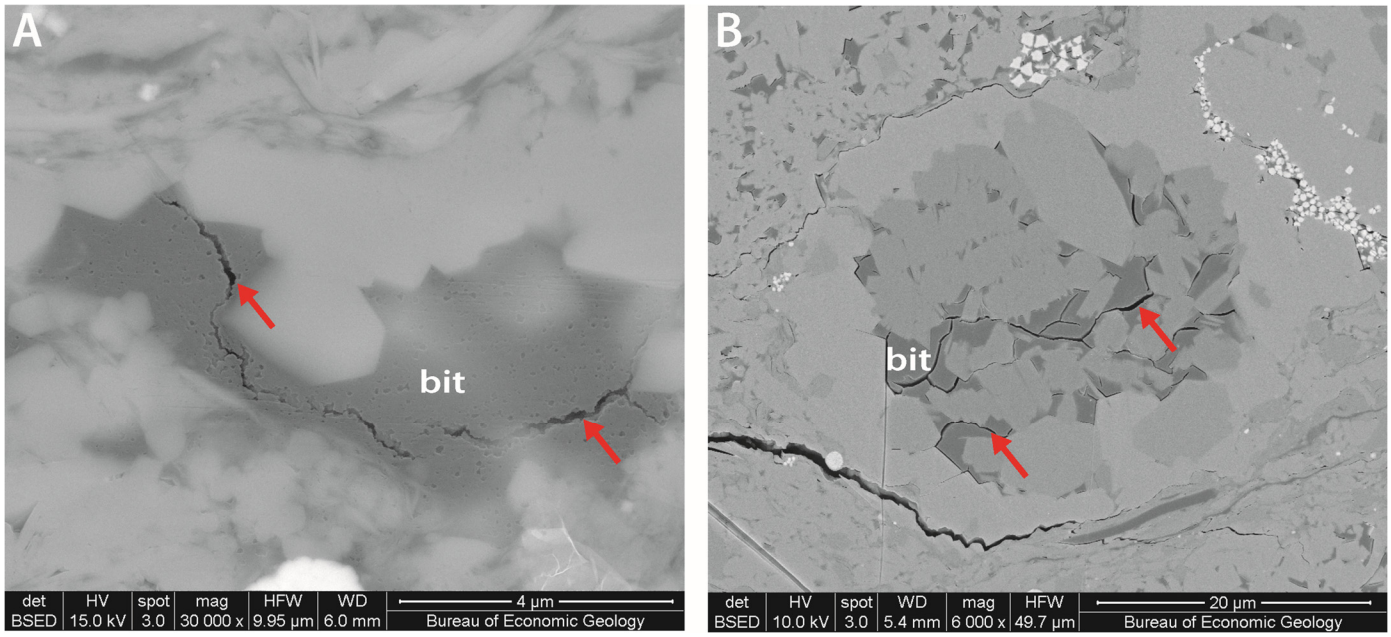

Figure 7. Backscattered electron SEM images of microfractures in organic matter. (A) En-echelon microfractures (red arrows) in bitumen (bit) consisting of linear arrangements of connected bubble pores. Permian Wolfcamp Shale, Reeves County, Texas, calculated R_o = ~0.9%. (B) Straight-sided microfractures (red arrows) in bitumen (bit) within a foraminifer chamber, probably postcoring in origin. Upper Cretaceous Eagle Ford Group, Gonzales County, Texas, calculated R_o = ~0.75%.

pores in some rare cases. Most challenging is the differentiation of pore types that are present in kerogen. The wide variability in inherited (predepositional) pore morphologies (Ko et al., 2016; Reed, 2017) adds to the difficulty. Some have questioned whether organic-matter pores related to thermal maturity even occur in kerogen (e.g., Bernard et al., 2012). However, the widespread occurrence of pores in kerogen from the thermally mature Barnett Shale (Loucks et al., 2009; Reed et al., 2014) coupled with the absence of pores in kerogen from the immature Barnett Shale (Reed and Loucks, 2015) argues against this hypothesis.

Differentiation of modified mineral pores from bubble pores can be challenging when bubble pores have not merged and remain more spherical. Modified mineral pores in larger original mineral pores also tend to be larger (> micrometer), although in smaller mineral pores they are smaller (< micrometer), similar to bubble pores. Observations suggest that modified mineral pores tend to have smooth organic-matter walls, whereas bubble pores have rougher walls. It is thought that modified mineral pores are more likely to be isolated, whereas bubble pores form in groups or aggregates. Modified mineral pores are also present in relatively immature mudrocks, if thermal maturity is sufficient to generate bitumen that migrates.

Other Issues

An additional challenge can be differentiating kerogen from solid bitumen in the SEM (Loucks and Reed, 2014; Milliken et al., 2014). This differentiation is complicated by the potential for kerogen to transform into bitumen in place during thermal maturity and causing the two organic matter types to become intermingled.

We think that at least six types of pores exist. Does this mean that additional types may be found? Such a possibility exists as organic matter from new regions and formations continues to be examined. A choice between separating similar morphologies of pores between kerogen and bitumen into separate pore types also exists, which has not been done in this investigation. Perhaps in the future that such a separation will become appropriate.

CONCLUSIONS

At least six distinct types of pores are associated with organic matter in mudrocks and are widespread enough to be significant: (1) inherited (predepositional) pores in kerogen (Fig. 1), (2) subgrain (granular) pores in kerogen (Fig. 2), (3) modified mineral pores associated with solid bitumen (Fig. 3), (4) bubble pores (Fig. 4), (5) spongy pores (Fig. 5), and (6) clay-shaped dissolution pores in organic matter (Fig. 6). Only two of these pore types clearly form in response to thermal maturation of the organic matter itself—bubble and spongy pores. Inherited pores suggest the presence of terrestrial kerogen. Modified mineral pores provide evidence of mobility of bitumen at low thermal maturity. Dissolution pores in organic matter provide evidence for late-stage diagenetic reactions involving clay minerals.

Some microfractures in organic matter (those composed of aligned connected pores) are thought to be naturally occurring. These are relatively rare and are confined to the organic-matter mass or grain in which they form. Straight-sided microfractures that can have curved traces in solid bitumen are thought to be devolatilization products that are post-coring in origin.

Only bubble and spongy pores are generally common enough to be considered important in storage and flow of hydrocarbons in most units. Other types of organic-matter pores provide important insights into the origin of organic matter and the organic-matter thermal history within mudrocks.

ACKNOWLEDGMENTS

This research was partly funded by the Mudrock Systems Research Laboratory at the Bureau of Economic Geology, Jackson School of Geosciences, University of Texas at Austin. Sponsoring companies include Anadarko, Apache, Aramco Services, BHP, BP, Cenovus, Centrica, Chesapeake, Cima, Cimarex,

Chevron, Concho, ConocoPhillips, Cypress, Devon, Encana, ENI, EOG, Equinor, EXCO, ExxonMobil, FEI, Geosun, Hess, Husky, IMP, Kerogen, Marathon, Murphy, Newfield, Oxy, Penn Virginia, Penn West, Pioneer, QEP, Repsol, Samson, Shell, Sinopec, Talisman, TecPetrol, Texas American Resources, The Unconventionals, University Lands, US EnerCorp, Valence, and YPF. Additionally, some funding was supplied by the State of Texas Advanced Resource Recovery (STARR) Project at the Bureau of Economic Geology. Funding for some study of the Vaca Muerta Formation was provided by Chevron.

Helpful reviews by Sven Egenhoff and Joan Spaw improved this manuscript. Technical editing was supplied by Lana Dieterich. The Media Group at the Bureau of Economic Geology is thanked for graphics support. Peter Eichhubl is thanked for supplying the Monterey Shale sample. Patrick Smith and Priyanka Periwal are thanked for assistance with sample preparation. Publication was authorized by the Director, Bureau of Economic Geology, Jackson School of Geosciences, University of Texas at Austin.

REFERENCES CITED

Bernard, B., R. Wirth, A. Schreiber, H. Schultz, and B. Horsfield, 2012, Formation of nanoporous pyrobitumen residues during maturation of the Barnett Shale (Fort Worth Basin): International Journal of Coal Geology, v. 103, p. 3–11, <https://doi.org/10.1016/j.coal.2012.04.010>.

Curtis, M. E., R. J. Ambrose, C. H. Sondergeld, and C. S. Rai, 2010, Structural characterization of gas shales on the micro- and nanoscales: Society of Petroleum Engineers Paper SPE–137693–MS, Richardson, Texas, 15 p., <https://doi.org/10.2118/137693-MS>.

Curtis, M. E., R. Ambrose, C. Sondergeld, and C. Rai, 2011, Transmission and scanning electron microscopy investigation of pore connectivity of gas shales on the nanoscale: Society of Petroleum Engineers Paper SPE–144391–MS, Richardson, Texas, 10 p., <https://doi.org/10.2118/144391-MS>.

Curtis, M. E., E. T. Goergen, J. Jernigen, C. Sondergeld, and C. Rai, 2014, Mapping organic matter distribution on the centimeter scales with nanometer resolution, Unconventional Resources Technology Conference Paper 1922757, Denver, Colorado, 8 p., <https://doi.org/10.15530/URTEC-2014-1922757>.

Driskill, B., N. Suurmeyer, S. Rilling-Hall, A. Govert, and A. Garbowicz, 2012, Reservoir description of the subsurface Eagle Ford Formation, Maverick Basin area, South Texas, USA: Society of Petroleum Engineers Paper SPE–154528–MS, 23 p., <https://doi.org/10.2118/154528-MS>.

Driskill, B., J. Walls, S. W. Sinclair, and J. DeVito, 2013, Applications of SEM imaging to reservoir characterization in the Eagle Ford Shale, South Texas, U.S.A, *in* W. Camp, E. Diaz, and B. Wawak, eds., Electron microscopy of shale hydrocarbon reservoirs: American Association of Petroleum Geologists Memoir 102, Tulsa, Oklahoma, p. 115–136.

Fishman, N. S., P. C. Hackley, H. A. Lowers, R. J. Hill, S. O. Egenhoff, D. D. Eberl, and A. E. Blum, 2012, The nature of porosity in organic-rich mudstones of the Upper Jurassic Kimmeridge Clay Formation, North Sea, offshore United Kingdom: International Journal of Coal Geology, v. 103, p. 32–50, <https://doi.org/10.1016/j.coal.2012.07.012>.

Jennings, D. S., and J. Antia, 2013, Petrographic characterization of the Eagle Ford Shale, South Texas: Mineralogy, common constituents, and distribution of nanometer-scale pore types, *in* W. Camp, E. Diaz, and B. Wawak, eds., Electron microscopy of shale hydrocarbon reservoirs: American Association of Petroleum Geologists Memoir 102, Tulsa, Oklahoma, p. 101–113.

Katz, B. J., and I. Arango, 2018, Organic porosity: A geochemist's view of the current state of understanding: Organic Geochemistry, v. 123, p. 1–16, <https://doi.org/10.1016/j.orggeochem.2018.05.015>.

Ko, L. T., R. G. Loucks, T. Zhang, S. C. Ruppel, and D. Shao, 2016, Pore and pore network evolution of Upper Cretaceous Boquillas (Eagle Ford-equivalent) mudrocks: Results from gold-tube pyrolysis experiments: American Association of Petroleum Geologists Bulletin, v. 100, p. 1693–1722, <https://doi.org/10.1306/04151615092>.

Ko, L. T., R. G. Loucks, S. C. Ruppel, T. Zhang, and S. Peng, 2017, Origin and characterization of Eagle Ford pore networks in the South Texas Upper Cretaceous shelf: American Association of Petroleum Geologists Bulletin, v. 101, p. 387–418, <https://doi.org/10.1306/08051616035>.

Liu, X., J. Xiong, and L. Liang, 2015, Investigation of pore structure and fractal characteristics of organic-rich Yanchang formation shale in central China by nitrogen adsorption/desorption analysis: Journal of Natural Gas Science and Engineering, v. 22, p. 62–72, <https://doi.org/10.1016/j.jngse.2014.11.020>.

Loucks, R. G., R. M. Reed, S. C. Ruppel, and D. M. Jarvie, 2009, Morphology, genesis, and distribution of nanometer-scale pores in siliceous mudstones of the Mississippian Barnett Shale: Journal of Sedimentary Research, v. 79, p. 848–861, <https://doi.org/10.2110/jsr.2009.092>.

Loucks, R. G., R. M. Reed, S. C. Ruppel, and U. Hammes, 2012, Spectrum of pore types and networks in mudrocks and a descriptive classification for matrix-related mudrock pores: American Association of Petroleum Geologists Bulletin, v. 96, p. 1071–1098, <https://doi.org/10.1306/08171111061>.

Loucks, R. G., and R. M. Reed, 2014, Scanning-electron-microscope petrographic evidence for distinguishing organic-matter pores associated with depositional organic matter versus migrated organic matter in mudrocks: Gulf Coast Association of Geological Societies Journal, v. 3, p. 51–60, <http://www.gcags.org/Journal/2014.GCAGS.Journal/GCAGS.Journal.2014.vol3.p51-60.Loucks.and.Reed.pdf>.

Loucks, R. G., and R. M. Reed, 2016, Natural microfractures in unconventional shale-oil and shale-gas systems: Real, hypothetical, or wrongly defined?: Gulf Coast Association of Geological Societies Journal, v. 5, p. 64–72, <http://www.gcags.org/Journal/2016.GCAGS.Journal/2016.GCAGS.Journal.v5.04.p64-72.Loucks.and.Reed.pdf>.

Loucks, R. G., R. M. Reed, L. T. Ko, J. Birdwell, S. T. Paxton, K. J. Whidden, and P. Hackley, 2019, Insights into early reservoir development of the Upper Cretaceous Eagle Ford Group and Pepper Shale from observations of the USGS Gulf Coast #1 West Woodway low–R_o research core in McLennan County, Central Texas (abs.): GeoGulf Transactions, v. 69, p. 551–552.

Miki, T., Y. Nakamuta, and J. Aizawa, 1991, Relationships between authigenic mineral transformation and variation of vitrinite reflectance during diagenesis; an example from the Tertiary of northern Kyushu, Japan: Clay Minerals, v. 26, p. 179–187, <https://doi.org/10.1180/claymin.1991.026.2.03>.

Milliken, K. L., 2005, Chapter 7. Elemental transfer in sandstone-shale sequences, *in* T. Mackenzie, ed., Treatise on geochemistry, v. 7: Sediments, diagenesis, and sedimentary rocks: Elsevier B.V., The Netherlands, p. 159–190.

Milliken, K. L., M. Rudnicki, D. N. Awwiller, and T. Zhang, 2013, Organic matter–hosted pore system, Marcellus Formation (Devonian), Pennsylvania: American Association of Petroleum Geologists Bulletin, v. 97, p. 177–200, <https://doi.org/10.1306/07231212048>.

Milliken, K. L., L. T. Ko, M. Pommer, and K. M. Marsaglia, 2014, SEM petrography of eastern Mediterranean sapropels: Analogue data for assessing organic matter in oil and gas shales: Journal of Sedimentary Research, v. 84, p. 961–974, <https://doi.org/10.2110/jsr.2014.75>.

Orr, W. L., 1986, Kerogen/asphaltene/sulfur relationships in sulfur-rich Monterey oils: Organic Geochemistry, v. 10, p. 499–516, <https://doi.org/10.1016/0146-6380(86)90049-5>.

Papp, A. P., J. C. Hower, and D. C. Peters, eds., 1998, Atlas of coal geology: American Association of Petroleum Geologists Studies in Geology 45, Tulsa, Oklahoma, CD–ROM publication.

Peng, S., R. M. Reed, X. Xiao, Y. Yang, and Y. Liu, 2019, Tracer-guided characterization of dominant pore networks and implications for permeability and wettability in shale: Journal of Geo-

physical Research: Solid Earth, v. 124, p. 1459–1479, <https://doi.org/10.1029/2018JB016103>.

Pommer, M., and K. L. Milliken, 2015, Pore types and pore-size distributions across thermal maturity, Eagle Ford Formation, southern Texas: American Association of Petroleum Geologists Bulletin, v. 99, p. 1713–1744, <https://doi.org/10.1306/03051514151>.

Reed, R. M., and R. G. Loucks, 2007, Imaging nanoscale pores in the Mississippian Barnett Shale of the northern Fort Worth Basin (abs.): American Association of Petroleum Geologists Search and Discovery Article 90063, Tulsa, Oklahoma, 1 p., <http://www.searchanddiscovery.com/abstracts/html/2007/annual/abstracts/lbReed.htm>.

Reed, R. M., R. G. Loucks, and S. C. Ruppel, 2014, Comment on "Formation of nanoporous pyrobitumen residues during maturation of the Barnett Shale (Fort Worth Basin)" by Bernard et al. (2012): International Journal of Coal Geology, v. 127, p. 111–113, <http://doi.org/10.1016/j.coal.2013.11.012>.

Reed, R. M., and R. G. Loucks, 2015, Low-thermal-maturity (<0.7% VR) mudrock pore systems: Mississippian Barnett Shale, southern Fort Worth Basin: Gulf Coast Association of Geological Societies Journal, v. 4, p. 15–28, <http://www.gcags.org/Journal/2015.GCAGS.Journal/2015.Journal.v4.2.p15-28.Reed.and.Loucks.press.pdf>.

Reed, R. M., and R. S. Roush, 2016, Pore systems of the Cline Shale, Midland Basin, West Texas: Unconventional Resources Technology Conference Paper 2423781, San Antonio, Texas, 10 p., <https://doi.org/10.15530-urtec-2016-2423781>.

Reed, R. M., 2017, Organic-matter pores: New findings from lower-thermal-maturity mudrocks: Gulf Coast Association of Geological Societies Journal, v. 6, p. 99–110, <http://www.gcags.org/Journal/2017.GCAGS.Journal/2017.GCAGS.Journal.v6.07.p99-110.Reed.pdf>.

Reed, R. M., J. E. Sivil, X. Sun, and S. C. Ruppel, 2019, Heterogeneity of microscale lithology and pore systems in an Upper Cretaceous Eagle Ford Group horizontal core, South Texas, USA: Gulf Coast Association of Geological Societies Journal, v. 8, p. 22–34, <http://www.gcags.org/Journal/2019.GCAGS.Journal/2019.GCAGS.Journal.v8.02.p22-34.Reed.et.al.pdf >.

Schieber, J., 1996, Early diagenetic silica deposition in algal cysts and spores: A source of sand in black shales?: Journal of Sedimentary Research, v. 66, p. 175–183, <https://doi.org/10.1306/d42682ed-2b26-11d7-8648000102c1865d>.

Yang, F., Z. Ning, H. Liu, 2014, Fractal characteristics of shales from a shale gas reservoir in the Sichuan Basin, China: Fuel, v. 115, p. 378–384, <https://doi.org/10.1016/j.fuel.2013.07.040>.